

**KINETICS OF CRYSTALLIZATION OF AMORPHOUS ALUMINA AND PHASE TRANSITION OF GAMMA-ALUMINA.** K. Kobayashi<sup>1</sup>, D. Yamamoto<sup>2</sup>, A. Takigawa<sup>3</sup>, and S. Tachibana<sup>3</sup>, <sup>1</sup>Hokkaido University, Japan, <sup>2</sup>Kyushu University, Japan (yamamoto.daiki.182@m.kyushu-u.ac.jp), <sup>3</sup>The University of Tokyo, Japan.

**Introduction:** Infrared spectroscopic observations have shown that amorphous and/or transition alumina ( $\text{Al}_2\text{O}_3$ ) rather than crystalline alumina (corundum) is present as a dominant dust phase around many AGB stars [e.g., 1]. On the other hand, corundum is the most major presolar alumina phase in primitive meteorites and only a few amorphous and transition alumina grains were reported [2, 3]. The presolar alumina grains examined their crystal structures were mostly identified in acid residues of meteorites, but amorphous and transition alumina is readily dissolved during acid treatments of meteorites [3], resulting in biased sampling of presolar alumina phases. Therefore, there could be a variety of presolar alumina phases, not identified yet, or there was a variety of alumina phases as dust in the protosolar disk but such a variety had lost during the solar system formation due to phase transition by heating and/or isotopic homogenization in the protosolar disk, which changes the relative abundance of different alumina phases in chondrites and the survivability of presolar alumina phases in the disk and/or during the chemical treatment of chondrites.

In this study, we conducted a series of annealing experiments on amorphous alumina to investigate kinetics of crystallization of amorphous alumina and that of phase transition of transition alumina.

**Experiments:** Micrometer-sized amorphous alumina grains, which was produced by drying a sol-gel synthesis alumina gel, were used as a starting material. The gel is identical to that synthesized in [3]. The gel was dried at 773 K for 2 h to obtain the most dehydrated-decarbonated amorphous without crystallization.

Heating experiments in air were conducted for crystallization of amorphous alumina at 943–1173 K for 2–288 h and for phase transition from  $\gamma$ -alumina to  $\alpha$ -alumina ( $\gamma$ - $\alpha$  phase transition) at 1173–1323 K for 1–912 h in one-atmosphere muffle furnaces (Nitto NHK-170AF, AS ONE HPM-ON). The alumina gel and run products were analyzed with Fourier transform infrared spectroscopy (FT-IR; JASCO FT-IR 4200), X-ray powder diffraction (XRD; Rigaku RINT-2100), and a scanning electron microscope (SEM; JEOL JCM-7000 NeoScope). Weight changes were measured with an ultra-microbalance (Mettler Toledo XP2U). After heating of amorphous alumina at 1173 K for 6 h and 1373 K for 12 h,  $\gamma$ - and  $\alpha$ -alumina formed, respectively, and were used as references to evaluate the degree of crystallization and phase transition of the samples. Note that neither phase transition nor further crystallization

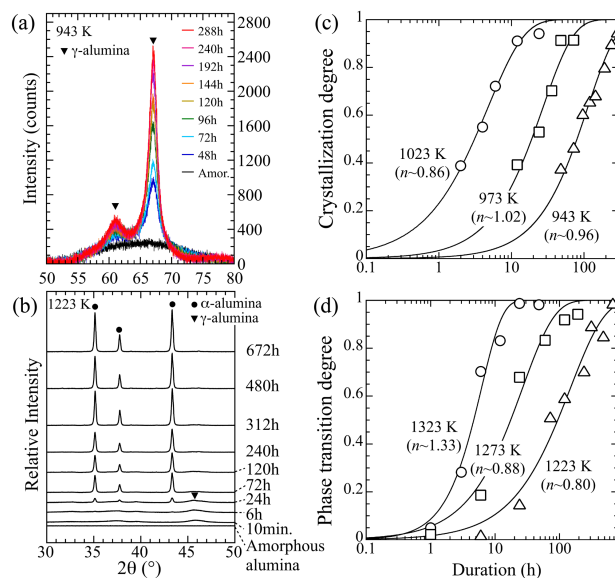


Fig. 1. (a) XRD profiles of the samples heated at 943 K. (b) XRD profiles of the samples heated at 1223 K. (c) Temporal changes of the crystallization degree at 943–1023 K. (d) Temporal changes of the degree of  $\gamma$ - $\alpha$  phase transition at 1223–1323 K.

was observed after heating for longer duration at these conditions.

**Results: Crystallization from amorphous alumina.**

Figure 1(a) shows an example of time-variant XRD patterns of the samples heated at 943 K in the range of 50–80° in  $2\theta$ . Peaks at 61 and 67° in  $2\theta$  due to  $\gamma$ -alumina gradually appeared from the original halo pattern of the amorphous alumina upon heating. Other transition alumina phases were not observed. The weight losses of the samples heated for the shortest duration reached ~5 wt%, and further changes in weight losses for the longer duration were not observed. These results suggest that residual volatile materials in the starting materials evaporated almost completely during the very early stage of crystallization.

**$\gamma$ - $\alpha$  phase transition.** The change in the XRD profiles of the samples heated at 1223 K for 10 min–672 h is shown in Fig. 1(b). Only broad peaks of  $\gamma$ -alumina were detected for 10 min–6 h and small peaks of  $\alpha$ -alumina appeared after 24 h-heating. After further heating, the broad peaks of  $\gamma$ -alumina gradually disappeared, and eventually only sharp peaks of  $\alpha$ -alumina were detected. Similar time evolution of the XRD peaks was observed at 1273 and 1323 K.

**Discussion:** Present results show that amorphous alumina first crystallizes into  $\gamma$ -alumina, which turns

into  $\alpha$ -alumina by higher temperature heating (Fig. 1). We thus evaluate the kinetics of crystallization of amorphous alumina and that of  $\gamma$ - $\alpha$  phase transition independently.

We quantitatively evaluated degrees of crystallization of amorphous alumina using XRD patterns at 50–80° in  $2\theta$  (Fig. 1(a)) and that of  $\gamma$ - $\alpha$  phase transition using XRD profiles at 43–44° in  $2\theta$  (Fig. 1(b)). Mixtures of the amorphous alumina and the  $\gamma$ -alumina references and those of  $\gamma$ -alumina and  $\alpha$ -alumina references with the mass ratios of 0.25, 0.5, and 0.75 were prepared and their XRD patterns were measured. The degrees of crystallization and phase transition were estimated from a linear correlation between areas of the XRD peaks and the mass ratio in the mixtures.

Temporal changes in the degree of crystallization/phase transition ( $x$ ) were well fitted with the Johnson-Mehl-Avrami equation ( $x = 1 - \exp(-(t/\tau)^n)$ ) where  $t$  is heating duration,  $\tau$  is the time constant for the crystallization/phase transition,  $n$  is the Avrami parameter which depends on the mechanism of the crystallization/phase transition (Fig. 1(c, d)). The estimated values of  $n$  were close to 1 for both crystallization and phase transition (Fig. 1(c, d)). In the case of crystallization,  $n$  is expected to be larger than 1 for crystallization associated with nucleation. The  $n \sim 1$  in this study indicates that residual water molecules in the starting material synthesized by the sol-gel method may help the nucleation of  $\gamma$ -alumina at the initial stage of crystallization. Regarding phase transition,  $n \sim 1$  is consistent with that in [4].

The Arrhenius plot of the  $\tau$  for crystallization and phase transition (Fig. 2) shows that crystallization of amorphous alumina precedes the  $\gamma$ - $\alpha$  phase transition and amorphous alumina transforms into  $\alpha$ -alumina via formation of  $\gamma$ -alumina in a wide range of temperature (Fig. 1(b)). The rate of  $\gamma$ - $\alpha$  phase transition in this study is consistent with those obtained at higher temperatures in previous experiments [4, 5] (Fig. 2)

The reaction temperatures (reaction lines) of crystallization and phase transition of alumina dust in steady accretion protoplanetary disks are calculated based on the reaction kinetics (details are described in [6]) (Fig. 3). Figure 3 also shows the oxygen isotope exchange lines of 1 micron-sized amorphous- and  $\gamma$ -alumina dust with disk gas based on O diffusivity [7]. Oxygen isotope exchange with amorphous- and  $\gamma$ -alumina tends to precede crystallization and phase transition in accreting disks. This suggests that if isotopically anomalous alumina grains were present in the form of amorphous or transition alumina, its original isotopic signature would be erased in the disk. The presolar alumina grains may thus be mostly present as

$\alpha$ -alumina if they were present in the accreting disk. The exception is 1-micron sized  $\gamma$ -alumina dust in the disk with the viscous parameter  $\alpha > 5 \times 10^{-3}$ ; dust may transform into  $\alpha$ -alumina without complete O isotope exchange. Such dust is likely to be recognized as a presolar corundum grain.

**References:** [1] Takigawa A. et al. (2019) *ApJL*, 878, L7 (8pp). [2] Stroud R. M. et al. (2004) *Science*, 305, 1455–1457. [3] Takigawa A. et al. (2014) *GCA*, 124, 309–327. [4] Yamaguchi O. et al. (1976) *J. Jpn Soc. Powder Metallurgy*, 23, 143–148. [5] McArdle J. L. and Messing G. L. (1993) *J. Am. Ceram. Soc.*, 76, 214–22. [6] Ishizaki L. et al. (2023) *This conference*. [7] Nabatame T. et al. (2003) *Jpn. J. Appl. Phys.*, 42, 7205–7208.

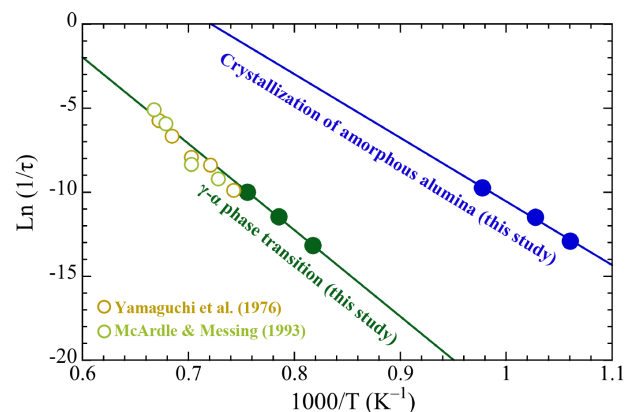


Fig. 2. Arrhenius plots of the reciprocal time constant ( $\tau$ ) for crystallization of amorphous alumina and  $\gamma$ - $\alpha$  phase transition.  $\tau$  for  $\gamma$ - $\alpha$  phase transition obtained in previous studies [4, 5] are also shown for comparison.

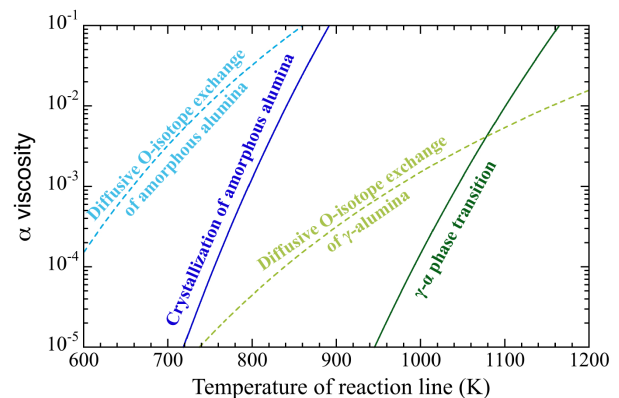


Fig. 3. Temperatures of crystallization of amorphous alumina and phase transition of  $\gamma$ -alumina in steady accreting protoplanetary disks with the  $\alpha$ -viscosity of  $10^{-1}$ – $10^{-5}$  and an accretion rate of  $10^{-7} M_{\text{sun}} \text{ yr}^{-1}$  calculated based on [6]. Temperatures required for oxygen isotopic exchange of 1  $\mu\text{m}$ -diameter amorphous and  $\gamma$ -alumina [7] are also shown for comparison.